Journal of Power Sources 267 (2014) 560–565

Contents lists available at ScienceDirect

Journal of Power Sources

journal homepage: www.elsevier.com/locate/jpowsour

4-(Trifluoromethyl)-benzonitrile: A novel electrolyte additive for lithium nickel manganese oxide cathode of high voltage lithium ion battery

Wenna Huang [a], Lidan Xing [a, *], Yating Wang [a], Mengqing Xu [a], Weishan Li [a, *], Fengchao Xie [b], Shengan Xia [b]

[a] School of Chemistry and Environment, Key Laboratory of Electrochemical Technology on Energy Storage and Power Generation of Guangdong Higher Education Institutes, Engineering Research Center of Materials and Technology for Electrochemical Energy Storage (Ministry of Education), South China Normal University, Guangzhou 510006, China

[b] Watt Laboratory, Huawei Technologies Co., Ltd., Shenzhen 518129, China

HIGHLIGHTS

- 4-TB is used as a novel electrolyte additive for high voltage lithium ion battery.
- Cyclic stability of $LiNi_{0.5}Mn_{1.5}O_4$ is improved significantly by using 4-TB.
- 4-TB is oxidized preferably to carbonate solvents forming a low-impedance protective film.
- The film suppresses subsequent decompositions of electrolyte and $LiNi_{0.5}Mn_{1.5}O_4$.

GRAPHICAL ABSTRACT

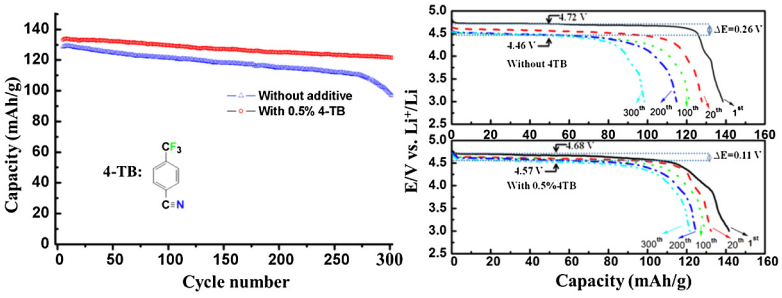

ARTICLE INFO

Article history:
Received 25 March 2014
Received in revised form
5 May 2014
Accepted 26 May 2014
Available online 4 June 2014

Keywords:
4-(Trifluoromethyl)benzonitrile
Electrolyte additive
Cyclic stability
High voltage lithium ion battery

ABSTRACT

In this work, 4-(Trifluoromethyl)-benzonitrile (4-TB) is used as a novel electrolyte additive for $LiNi_{0.5}Mn_{1.5}O_4$ cathode of high voltage lithium ion battery. Charge–discharge tests show that the cyclic stability of $LiNi_{0.5}Mn_{1.5}O_4$ is significantly improved by using 0.5 wt.% 4-TB. With using 4-TB, $LiNi_{0.5}Mn_{1.5}O_4$ delivers an initial capacity of 133 mAh g^{-1} and maintains 121 mAh g^{-1} after 300 cycles with a capacity retention of 91%, compared to the 75% of that using base electrolyte (1 M $LiPF_6$ in ethylene carbonate(EC)/dimethyl carbonate(DMC)). The results from linear sweep voltammetry, density functional theory calculations, electrochemical impedance spectroscopy, scanning electron microscope, energy dispersive spectroscopy, Fourier transform infrared, and inductively coupled plasma, indicate that 4-TB has lower oxidative stability than EC and DMC, and is preferentially oxidized on $LiNi_{0.5}Mn_{1.5}O_4$ forming a low-impedance protective film, which prevents the subsequent oxidation decomposition of the electrolyte and suppresses the manganese dissolution from $LiNi_{0.5}Mn_{1.5}O_4$.

1. Introduction

Developments of lithium ion batteries with high energy density, high power density and low cost have aroused tremendous attention because of their potential application in energy storage for electric vehicles [1–4]. One of the efficient ways to increase the

* Corresponding authors. Tel./fax: +86 20 39310256.
E-mail addresses: xingld@scnu.edu.cn (L. Xing), liwsh@scnu.edu.cn (W. Li).

http://dx.doi.org/10.1016/j.jpowsour.2014.05.124
0378-7753/

energy density of lithium ion battery is to use cathode materials with high operating voltage (5 V vs. Li^+/Li) [5–7], such as $LiNiPO_4$ [8], $LiNiSO_4F$ [9] and $LiNi_{0.5}Mn_{1.5}O_4$ [10]. Unfortunately, the oxidative decomposition of the conventional carbonate-based electrolytes (>4.5 V, vs. Li^+/Li) and the dissolution of the cathode materials limit their applications in commercial lithium ion batteries [11].

Improving the oxidative stability of electrolytes becomes a high priority for the development of high voltage lithium ion batteries [12–15]. Solvents such as sulfones [14,16,17], ionic liquids [12,18] and dinitriles [19–21], and electrolyte additives [13,22–27] have been reported to be able to improve the cyclic stability of cathode for high voltage lithium ion batteries. For example, lithium bis(oxalato)borate(LiBOB)/Sulfolane/γ-butyrolactone/diethyl carbonate (DMC) electrolyte was shown to provide a high capacity retention of 85.9% for $LiNi_{0.5}Mn_{1.5}O_4$ after 100 cycles (0.5 C) [28]. Cresce and coworkers [24] reported that a highly fluorinated phosphate ester, tris(hexafluoro-iso-propyl)-phosphate, could improve the cyclic performance of $LiNi_{0.5}Mn_{1.5}O_4$, with a capacity retention of 87% after 200 cycles (0.5 C).

In this paper, we reported a novel electrolyte additive, 4-(Trifluoromethyl)benzonitrile (4-TB), with which a 1 C rate capacity retention of over 90% for $LiNi_{0.5}Mn_{1.5}O_4$ after 300 cycles is achieved. The mechanism on the improved cyclic stability of $LiNi_{0.5}Mn_{1.5}O_4$ by using 4-TB was illustrated.

2. Calculation and experimental

All calculations were performed using the Gaussian 09 package [29]. The equilibrium structures were optimized with the B3LYP in conjunction with the 6-311++G (d) level basis set [30]. Polarized continuum models (PCM) were used to investigate the bulk solvent effect (dielectric constant is 20.5). The calculated oxidation potential was converted from the Free-energy cycle for the oxidation reaction [31].

Battery-grade carbonate solvents and lithium hexafluorophosphate ($LiPF_6$) were provided by Guangzhou Tinci Materials Technology Co. Ltd., China. The additive, 4-TB (99%), was purchased from Sigma–Aldrich, and used without further purification. The base electrolyte was 1.0 M $LiPF_6$ in ethylene carbonate (EC)/DMC (1/2, in volume). The HF and water content in these solutions were less than 5 ppm. $LiNi_{0.5}Mn_{1.5}O_4$ electrode was prepared by mixing 80 wt.% $LiNi_{0.5}Mn_{1.5}O_4$, 10 wt.% acetylene carbon black, 5 wt.% Super-P and 5 wt.% PVDF binder and coating the mixture on Al foil. $Li/LiNi_{0.5}Mn_{1.5}O_4$ coin cells (size: 2025) with Celgard 2400 microporous membrane as the separator were assembled inside an Ar gas-filled glove box. The contents of water and oxygen in this grove box were controlled to less than 0.1 and 10 ppm, respectively.

Charge–discharge tests were performed at room temperature between 3.0 and 4.9 V using LAND cell test system (Land CT 2001A, China). The cells were cycled at a constant current–constant voltage charge to 4.9 V and a constant current discharge to 3.0 V. The cells were cycled at C/10 (1 C = 0.468 mA cm^{-2}) for the initial two cycles and 1 C for the remaining cycles. The electrochemical impedance spectroscopy (EIS) was performed on a frequency response analyzer (Metrohm Autolab PGSTAT302N, the Netherlands), with a frequency range from 100 kHz to 0.01 Hz, using an ac signal with 5 mV amplitude.

The electrodes for structure and composition characterizations were washed five times with anhydrous DMC to remove the residual solvents and $LiPF_6$ salt and dried in vacuum overnight at room temperature. Ex-situ scanning electron microscope (SEM) and Energy Dispersive Spectroscopy (EDS) analyses were conducted on a JEOL-5900 SEM. Inductively Coupled Plasma (ICP) was performed on an IRIS Intrepid II XSP. The samples for ICP analyses were made from the cycled lithium electrode, which were rinsed with anhydrous DMC and treated with 1 mL 2% HNO_3. Fourier transform infrared-attenuated total reflectance (FTIR-ATR) analysis was carried out with a Nicolet 6700 spectrometer.

3. Results and discussion

3.1. Improved cyclic stability of $LiNi_{0.5}Mn_{1.5}O_4$ by using 4-TB

Fig. 1 presents the cyclic performances of $Li/LiNi_{0.5}Mn_{1.5}O_4$ cells using electrolyte with and without 0.5 wt.% 4-TB. It can be seen from Fig. 1 that the cyclic stability of $LiNi_{0.5}Mn_{1.5}O_4$ is significantly improved by 4-TB. With using the additive, $LiNi_{0.5}Mn_{1.5}O_4$ delivers an initial capacity of 133 mAh g^{-1} and maintains 121 mAh g^{-1} after 300 cycles with a capacity retention of 91%, compared to the 75% of that using base electrolyte. The charge–discharge efficiency of the cell using 4-TB-containing electrolyte is 2% higher than the cell using base electrolyte at the 300th cycle, suggesting that the electrolyte decomposition happen less easily in the former than the latter. The efficiency of the cell with 4-TB (84.5%) is lower than that without additive (88.2%) in the first cycle at C/10, suggesting that 4-TB is oxidized when the cell is charged.

Fig. 2 presents the discharge curves of $LiNi_{0.5}Mn_{1.5}O_4$ electrodes with and without 4-TB. The potential plateau is corresponding to the Li^+ intercalation reaction of $LiNi_{0.5}Mn_{1.5}O_4$. It can be found that the plateau potential of $LiNi_{0.5}Mn_{1.5}O_4$ electrode without 4-TB decreases gradually with increasing cycle, from 4.72 (the 1st cycle) to 4.46 V (the 300th cycles), indicating that the polarization of lithium insertion/de-insertion in $LiNi_{0.5}Mn_{1.5}O_4$ increases during cycling. This increased polarization can be ascribed to the oxidative decomposition of carbonate solvents and shows the instability of the interface between the electrode and electrolyte. As for the $LiNi_{0.5}Mn_{1.5}O_4$ cycled in 4-TB-containing electrolyte, the plateau potential in the first cycle is about 0.04 V lower than that cycled in base electrolyte, revealing that the initial polarization of lithium insertion/de-insertion in $LiNi_{0.5}Mn_{1.5}O_4$ with 4-TB-contanining electrolyte is slightly larger than that with base electrolyte. This might result from the film formed from 4-TB. However, the plateau potential of $LiNi_{0.5}Mn_{1.5}O_4$ electrode with 4-TB-contanining electrolyte decreases more slowly than that with base electrolyte, dropping to only 4.57 V after 20 cycles and remaining constant after 300 cycles. This suggests that the interfacial stability between $LiNi_{0.5}Mn_{1.5}O_4$ and electrolyte can be improved by using 4-TB.

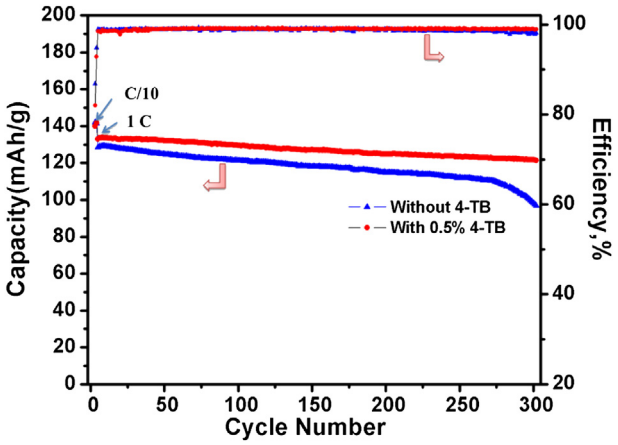

Fig. 1. Cyclic performances of the $Li/LiNi_{0.5}Mn_{1.5}O_4$ cells using electrolytes with and without 0.5% 4-TB (initial two cycles were performed at C/10, and the remaining cycles at 1 C). The cells were charged and discharged between 4.9 and 3.0 V.

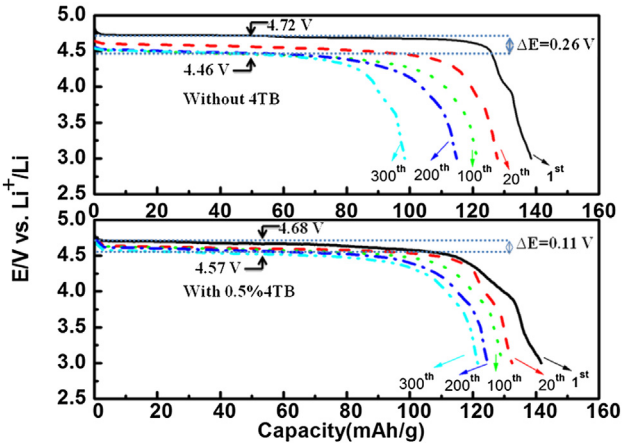

Fig. 2. Discharge curves of the Li/$LiNi_{0.5}Mn_{1.5}O_4$ cells using electrolytes with and without 0.5% 4-TB.

EIS was performed to understand the interfacial stability between $LiNi_{0.5}Mn_{1.5}O_4$ and electrolyte. Fig. 3 presents the obtained results, which are characteristic of a semicircle at high frequencies and a slope line at low frequencies. The semicircle reflects the interfacial properties between $LiNi_{0.5}Mn_{1.5}O_4$ and electrolyte, while the slope line represents the diffusion of lithium ion in the electrode [32]. The reaction resistance for lithium insertion/deinsertion can be estimated by the diameter of the semicircle. As shown in Fig. 3, before cycling, the interfacial resistance is similar for both electrodes with and without 4-TB and larger compared to the cycled electrode, which can be ascribed to the incompletely wetted interface between electrodes and electrolyte. For the cell cycled in base electrolyte, the interfacial resistance increases with increasing cycling from the 10th cycle, showing the instability of the interface between the electrode and electrolyte, which is in good agreement with the faster decrease in plateaus potential observed in Fig. 2. For the cell cycled in 4-TB-containing electrolyte, the interfacial resistance at 10 cycles (about 275 Ω) is higher than the cell cycled in base electrolyte (about 162 Ω), conforming to its larger initial polarization observed in Fig. 2. As the cycling is performed further, however, the interfacial resistance of the cell using 4-TB-containing electrolyte remains almost unchanged, confirming the interfacial stability of the electrode and electrolyte.

We proposed that the improved interfacial stability is ascribed to the film formed by 4-TB. 4-TB is oxidized preferably to the electrolyte forming a protective film on $LiNi_{0.5}Mn_{1.5}O_4$, which protects $LiNi_{0.5}Mn_{1.5}O_4$ from dissolution and suppresses the electrolyte decomposition. To understand the mechanism on the improved cyclic stability of the $LiNi_{0.5}Mn_{1.5}O_4$ by 4-TB, the oxidative stability of 4-TB was compared with those of the carbonate solvents in the electrolyte by density functional theory (DFT) calculation and linear sweep voltammetry methods. Surface properties of the cycled $LiNi_{0.5}Mn_{1.5}O_4$ and lithium electrodes were also identified.

3.2. Oxidative stability of 4-TB

According to our previous DFT work, we found that the presence of anion lowered the oxidative stability of the carbonate solvents [31,33]. Hence, the influence of anion (PF_6^-) was also considered in this work. The optimized structures are shown in Fig. 4, and the calculated oxidation potential and the highest occupied molecular orbital (HOMO)/lowest unoccupied molecular orbital (LUMO) energies are listed in Table 1. The HOMO energy of 4-TB (−0.2934) is

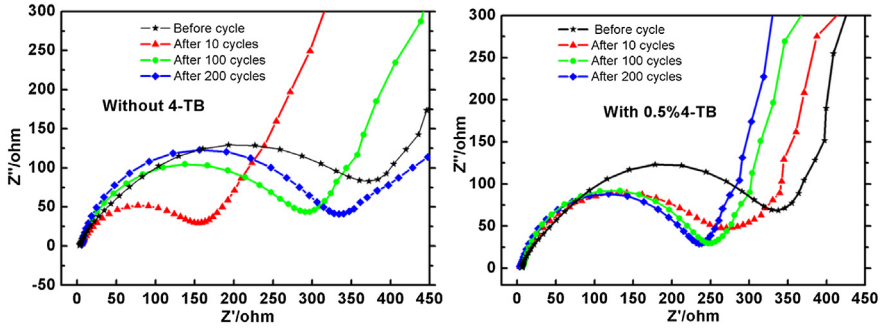

Fig. 3. Electrochemical impedance spectra of the cycled Li/$LiNi_{0.5}Mn_{1.5}O_4$ cells using electrolytes with and without 0.5% 4-TB.

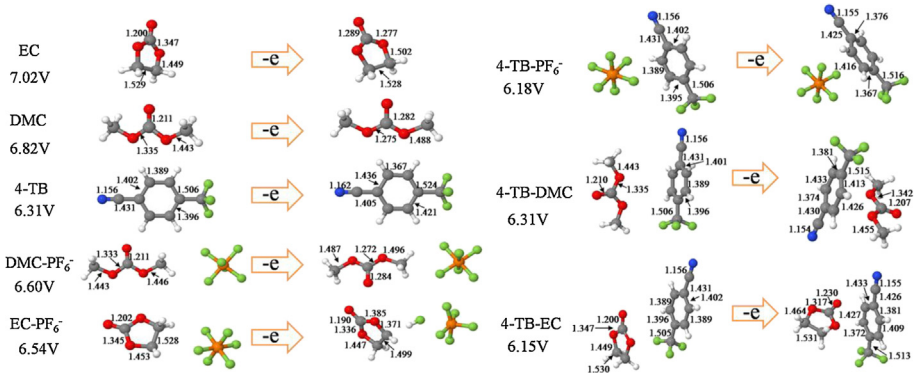

Fig. 4. Optimized structures and geometric parameters (bond length in Å) of the EC/DMC/4-TB-anion/solvent clusters before and after oxidation.

Table 1
Calculated oxidation potential (V vs. Li^+/Li) and HOMO/LUMO energies (au.) of EC, DMC and 4-TB.

Solvent	HOMO	LUMO	Calculated oxidation potential	
			Isolate	Solvent–PF_6^-
EC	−0.3209	−0.0075	7.02	6.54
DMC	−0.3180	−0.0071	6.82	6.60
4-TB	−0.2934	−0.0846	6.31	6.16

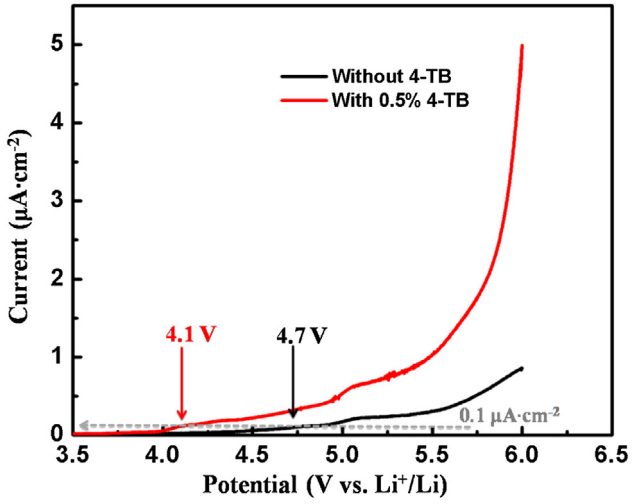

Fig. 5. Linear sweep voltammograms of Pt electrode in 1 mol L^{-1} $LiPF_6$ EC/DMC (1/2, in volume) with and without 0.5% 4-TB at 0.5 mV s^{-1}, OCV-6.0 V (vs. Li/Li^+).

less negative than EC (−0.3209) and DMC (−0.3180), indicating the lower oxidative stability of 4-TB than EC and DMC. Indeed, the calculated oxidation potentials of 4-TB (6.31 V) and 4-TB–PF_6^- (6.16 V) are lower than that of EC (7.02 V), DMC (6.82 V) and EC–PF_6^- (6.54 V), DMC–PF_6^- (6.60 V), respectively. Hence, preferential oxidative reaction of 4-TB in the $LiPF_6$/EC:DMC electrolyte can be expected.

These calculations are in good agreement with the results obtained from linear sweep voltammetry. Fig. 5 presents the linear sweep voltammograms of platinum in the electrolytes with and without 4-TB. The decomposition potentials of the electrolytes are determined at the value that the current densities reach 0.1 μA cm^{-2}. For the base electrolyte, the oxidation decomposition potential is around 4.7 V (vs. Li/Li^+). However, when adding 0.5 wt.% 4-TB, the oxidation decomposition potential decreases to around 4.1 V (vs. Li/Li^+), indicative of the preferential oxidation of 4-TB.

3.3. Surface morphology and compositions of $LiNi_{0.5}Mn_{1.5}O_4$ electrode

The surface morphologies of the $LiNi_{0.5}Mn_{1.5}O_4$ electrodes before and after cycled in the electrolyte with and without 4-TB were observed by SEM, the obtained results are shown in Fig. 6. For the electrode before cycling (see Fig. 6a), clear edges and smooth surface of $LiNi_{0.5}Mn_{1.5}O_4$ particles can be identified. The SEM images of the $LiNi_{0.5}Mn_{1.5}O_4$ electrode after 300 cycles without and with 4-TB are presented in Fig. 6b and c, respectively. It can be found that the $LiNi_{0.5}Mn_{1.5}O_4$ particles are separated into smaller ones when experiencing cycling in the base electrolyte. This can be ascribed to the Jahn–Teller crystallographic distortion

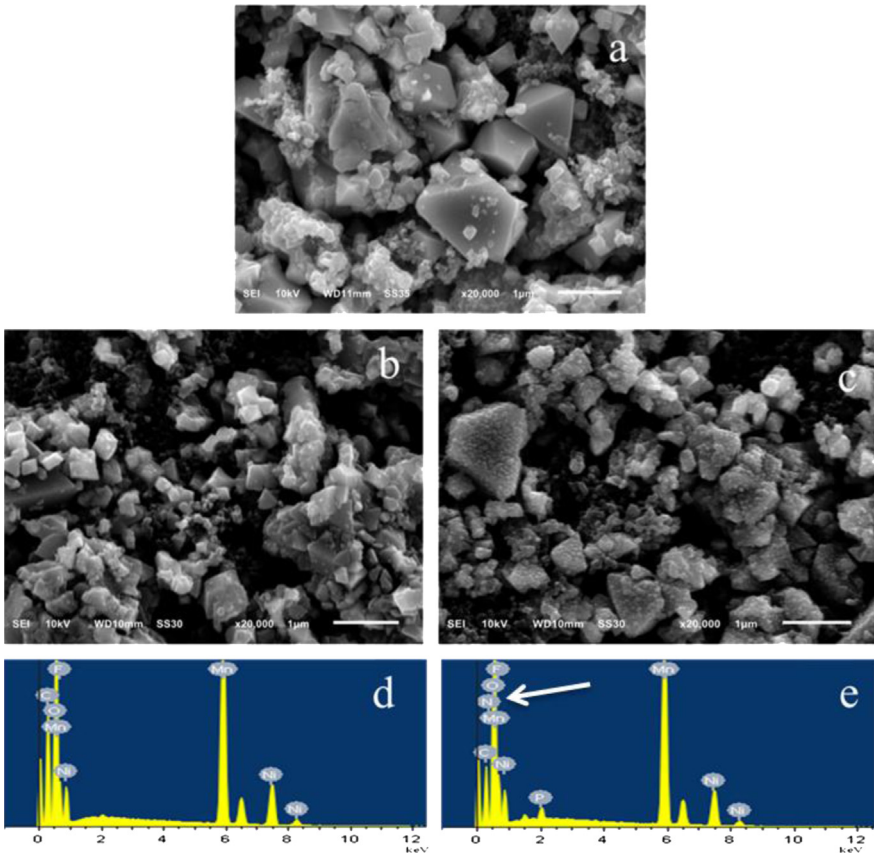

Fig. 6. SEM images of $LiNi_{0.5}Mn_{1.5}O_4$ electrodes: fresh (a), after the 300 cycles in 1.0 M $LiPF_6$/EC–DMC (1:2) without (b) and with 0.5% 4-TB (c). EDS spectra of $LiNi_{0.5}Mn_{1.5}O_4$ electrodes cycled in the electrolytes without (d) and with 0.5% 4-TB (e).

Table 2
Surface concentration of elements on $LiNi_{0.5}Mn_{1.5}O_4$ electrodes cycled with and without 0.5 wt.% 4-TB.

	C	O	F	Mn	Ni	N
Without 4-TB	25.68	30.60	8.05	26.32	9.34	–
With 4-TB	14.65	33.68	14.21	26.79	8.77	1.35

associated with the dissolution of $LiNi_{0.5}Mn_{1.5}O_4$ in electrolyte, resulting from the formation of Mn^{3+} ions [34]. The dissolution of $LiNi_{0.5}Mn_{1.5}O_4$ is extremely destructive to the cell life, because it not only breaks directly the cathode but also leads to the destruction of the anode through the deposition of the dissolved metal ions [34,35].

Differently, the $LiNi_{0.5}Mn_{1.5}O_4$ particles cycled in the 4-TB-containing electrolyte (see Fig. 6c) remains better similarity in morphology to the pristine particles than those cycled in the base electrolyte (Fig. 6b), indicating the addition of 4-TB could improve the structure stability of $LiNi_{0.5}Mn_{1.5}O_4$. Additionally, we found that the $LiNi_{0.5}Mn_{1.5}O_4$ particles cycled in the additive-containing electrolyte were apparently covered with a film, which should be generated from the oxidative reactions of 4-TB. Indeed, nitrogen element from 4-TB can be identified on the $LiNi_{0.5}Mn_{1.5}O_4$ cycled in the additive-containing electrolyte, as shown in Fig. 6e and Table 2. Moreover, the concentration of fluorine in the 4-TB containing system is higher than the base one, which may result from the $-CF_3$ group in 4-TB due to the incorporation of 4-TB oxidation decomposition products into the surface film.

Fig. 7 presents the FTIR spectra of pure 4-TB and $LiNi_{0.5}Mn_{1.5}O_4$ electrodes after cycled in the electrolyte with and without 4-TB. For the charged electrodes, the spectra around 1646, 1453, 1335, and 1095 cm^{-1} are corresponding to the vibration of C═O, Li_2CO_3, $ROCO_2Li$, and C–O, respectively [36,37], which result from the electrolyte decomposition. Importantly, a new broad peak around 2235 cm^{-1} can be observed on the cycled electrode in the 4-TB-containing electrolyte, which is corresponding to the vibration of Benzene–C≡N group [38]. This result confirms the incorporation of 4-TB oxidation decomposition products into the surface film.

With the results available, the mechanism on the formation of surface film by 4-TB can be inferred as follows. As the optimized structure of 4-TB before and after oxidation shown in Fig. 4, the benzene and C≡N groups remains unchanged after losing one electron, while the bond length of C(from C≡N)–C(from benzene) and C(from $-CF_3$)–C(from benzene) bond decreases and increases, respectively. Hence, a breakage reaction of the later after oxidation can be expected, generating a benzene–C≡N cation and CF_3 radical. The cation gains electron from surrounding solvents generating new radicals. All the radicals terminate and deposit on $LiNi_{0.5}Mn_{1.5}O_4$ surface forming a proactive surface film.

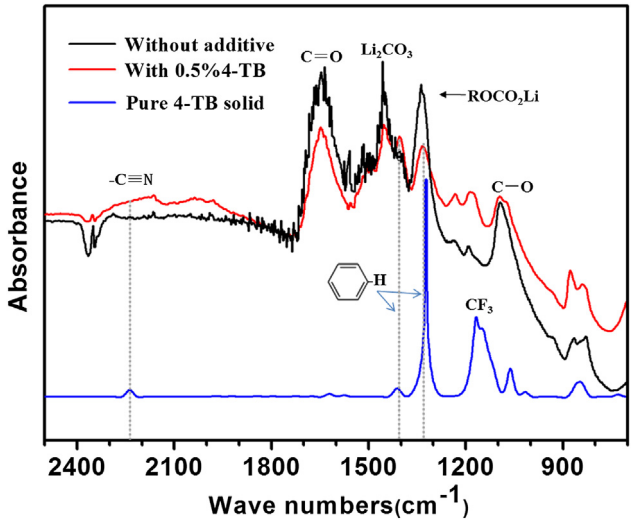

Fig. 7. FTIR spectra of pure 4-TB and $LiNi_{0.5}Mn_{1.5}O_4$ electrodes cycled in electrolyte with and without 0.5% 4-TB.

3.4. Deposition of dissolved metal ions on lithium electrode

To confirm the dissolution of the $LiNi_{0.5}Mn_{1.5}O_4$ and the subsequent deposition of the dissolved metal ions on the counter electrode during charging–discharging, composition of the lithium electrode taken from the cycled Li/$LiNi_{0.5}Mn_{1.5}O_4$ cell was analyzed with ICP. It is found that the content of Mn and Ni is 1.83 and 0.38 ppm for the electrode cycled in the base electrolyte, while drops to 0.85 and 0.26 ppm for the electrode cycled with 4-TB, respectively. Apparently, the dissolution of Mn and Ni ions from $LiNi_{0.5}Mn_{1.5}O_4$ and their subsequent deposition on the counter electrode do happen in the cycled cell. The less identified contents of Mn and Ni in the lithium electrode cycled with 4-TB indicates the film on $LiNi_{0.5}Mn_{1.5}O_4$ electrode formed by 4-TB is protective for $LiNi_{0.5}Mn_{1.5}O_4$ and suppresses the dissolution of Mn and Ni from $LiNi_{0.5}Mn_{1.5}O_4$.

4. Conclusions

4-TB is an effective film-forming additive for $LiNi_{0.5}Mn_{1.5}O_4$ based high voltage lithium ion battery. Addition of 0.5 wt.% 4-TB in the electrolyte of 1.0 M $LiPF_6$ in EC/DMC significantly improves the cyclic stability of $LiNi_{0.5}Mn_{1.5}O_4$. Theoretical and experimental results show that 4-TB is oxidized preferably to the carbonate solvents in the electrolyte, forming a protective film on $LiNi_{0.5}Mn_{1.5}O_4$, which suppresses the subsequent oxidation decomposition of the electrolyte and the dissolution of Mn and Ni from $LiNi_{0.5}Mn_{1.5}O_4$.

Acknowledgments

This work is supported by the National Natural Science Foundation of China (21303061 and 21273084), the Joint Project of the National Natural Science Foundation of China and the Natural Science Foundation of Guangdong (U1134002), the Natural Science Foundation of Guangdong Province (10351063101000001 and S2011040001731), and the Key Project of Science and Technology in Guangdong Province (2012A010702003).

References

[1] K. Xu, Chem. Rev. 104 (2004) 4303.
[2] W. Tang, Y.S. Zhu, Y.Y. Hou, L.L. Liu, Y.P. Wu, K.P. Loh, H.P. Zhang, K. Zhu, Energy Environ. Sci. 6 (2013) 2093.
[3] P. Zhang, G.C. Li, H.P. Zhang, L.C. Yang, Y.P. Wu, Electrochem. Commun. 11 (2009) 161.
[4] X.J. Wang, Q.T. Qu, Y.Y. Hou, F.X. Wang, Y.P. Wu, Chem. Commun. 49 (2013) 6179.
[5] J. Wolfenstine, J. Allen, J. Power Sources 142 (2005) 389.
[6] F. Zhou, X.M. Zhao, A.V. Bommel, X. Xia, J.R. Dahn, J. Electrochem. Soc. 158 (2011) A187.
[7] A. Kraytsberg, Y.E. Eli, Adv. Energy Mater. 2 (2012) 922.
[8] F. Zhou, M. Cococcioni, K. Kang, G. Ceder, Electrochem. Commun. 6 (2004) 1144.
[9] T. Mueller, G. Hautier, A. Jain, G. Ceder, Chem. Mater. 23 (2011) 3854.
[10] A. Manthiram, J. Phys. Chem. Lett. 2 (2011) 176.
[11] M. Hu, X.L. Pang, Z. Zhou, J. Power Sources 237 (2013) 229.
[12] X.W. Gao, C.Q. Feng, S.L. Chou, J.Z. Wang, J.Z. Sun, M. Forsyth, D.R. MacFarlane, H.K. Liu, Electrochim. Acta 101 (2013) 151.
[13] L. Zhang, Z.C. Zhang, H. Wu, K. Amine, Energy Environ. Sci. 4 (2011) 2858.
[14] K. Xu, C.A. Angell, J. Electrochem. Soc. 149 (2002) A920.

[15] K. Ariyoshi, Y. Iwakoshi, N. Nakayama, T. Ohzuku, J. Electrochem. Soc. 151 (2004) A296.
[16] S. Li, Y. Zhao, X. Shi, B. Li, X. Xu, W. Zhao, X. Cui, Electrochim. Acta 65 (2012) 221.
[17] A. Abouimrane, I. Belharouak, K. Amine, Electrochem. Commun. 11 (2009) 1073.
[18] S. Seki, Y. Ohno, H. Miyashiro, Y. Kobayashi, A. Usami, Y. Mita, N. Terada, K. Hayamizu, S. Tsuzuki, M. Watanabe, J. Electrochem. Soc. 155 (2008) A421.
[19] A.J. Gmitter, I. Plitz, G.G. Amatucci, J. Electrochem. Soc. 159 (2012) A370.
[20] Y.A. Lebdeh, I. Davidson, J. Power Sources 189 (2009) 576.
[21] M. Nagahama, N. Hasegawa, S. Okada, J. Electrochem. Soc. 157 (2010) A748.
[22] M.Q. Xu, Y.L. Liu, B. Li, W.S. Li, X.P. Li, S.J. Hu, Electrochem. Commun. 18 (2012) 123.
[23] M.Q. Xu, L. Zhou, Y.N. Dong, Y.J. Chen, A. Garsuch, B.L. Lucht, J. Electrochem. Soc. 160 (2013) A2005.
[24] A.V. Cresce, K. Xu, J. Electrochem. Soc. 158 (2011) A337.
[25] T. Kubota, M. Ihara, S. Katayama, H. Nakai, J. Ichikawa, J. Power Sources 207 (2012) 141.
[26] S.Y. Ha, J.G. Han, Y.M. Song, M.J. Chun, S. Il Han, W.C. Shin, N.S. Choi, Electrochim. Acta 104 (2013) 170.
[27] Z.D. Li, T.C. Zhang, H.F. Xiang, X.H. Ma, Q.F. Yuan, Q.S. Wang, C.H. Chen, J. Power Sources 240 (2013) 471.
[28] X.L. Cui, H.M. Zhang, S.Y. Li, Y.Y. Zhao, L.P. Mao, W. Zhao, Y.L. Li, X.S. Ye, J. Power Sources 240 (2013) 476.
[29] M.J. Frisch, G.W. Trucks, H.B. Schlegel, G.E. Scuseria, M.A. Robb, J.R. Cheeseman, G. Scalmani, V. Barone, B. Mennucci, G.A. Petersson, Gaussian 09, Revision A, Gaussian, Inc., Wallingford, CT, 2009.
[30] L.D. Xing, C.Y. Wang, W.S. Li, M.Q. Xu, X.L. Meng, S.F. Zhao, J. Phys. Chem. B 113 (2009) 5181.
[31] L.D. Xing, O. Borodin, Phys. Chem. Chem. Phys. 14 (2012) 12838.
[32] X.X. Zuo, C.J. Fan, X. Xiao, J.S. Liu, J.M. Nan, J. Power Sources 219 (2012) 94.
[33] L.D. Xing, O. Borodin, G.D. Smith, W.S. Li, J. Phys. Chem. A 115 (2011) 13896.
[34] B.Z. Li, L.D. Xing, M.Q. Xu, H.B. Lin, W.S. Li, Electrochem. Commun. 34 (2013) 48.
[35] B. Li, Y.Q. Wang, H.B. Rong, Y.T. Qang, J.S. Liu, L.D. Xing, M.Q. Xu, W.S. Li, J. Mater. Chem. A 1 (2013) 129541.
[36] K. Morigaki, A. Ohta, J. Power Sources 76 (1998) 159.
[37] P. Verma, P. Maire, P. Novák, Electrochim. Acta 55 (2010) 6332.
[38] E. Pretch, P. Bühlmann, M. Badertscher (Eds.), Structure Determination of Organic Compounds: Tables of Spectral Data, Springer, 2000, p. 299.